Structural and magnetic properties of In1-xMnxSb: Effect of Mn complexes and MnSb nanoprecipitates

AIP | Journal of Applied Physics

Structural and magnetic properties of In1−xMnxSb: Effect of Mn complexes and MnSb nanoprecipitates

A. V. Kochura, B. A. Aronzon, K. G. Lisunov, A. V. Lashkul, A. A. Sidorenko et al.

Citation: J. Appl. Phys. **113**, 083905 (2013); doi: 10.1063/1.4792652
View online: http://dx.doi.org/10.1063/1.4792652
View Table of Contents: http://jap.aip.org/resource/1/JAPIAU/v113/i8
Published by the American Institute of Physics.

JOURNAL OF APPLIED PHYSICS **113**, 083905 (2013)

Structural and magnetic properties of $In_{1-x}Mn_xSb$: Effect of Mn complexes and MnSb nanoprecipitates

A. V. Kochura,[1,2] B. A. Aronzon,[1,3,4] K. G. Lisunov,[1,5] A. V. Lashkul,[1] A. A. Sidorenko,[6,a)] R. De Renzi,[6] S. F. Marenkin,[7] M. Alam,[2] A. P. Kuzmenko,[2] and E. Lähderanta[1,b)]
[1]*Department of Mathematics and Physics, Lappeenranta University of Technology, PO Box 20, FIN-53851 Lappeenranta, Finland*
[2]*South-West State University, 50 let Oktjabrja Str., 305040 Kursk, Russia*
[3]*Russian Research Centre "Kurchatov Institute ", 1 Kurchatov Square, 123182 Moscow, Russia*
[4]*Institute of Theoretical and Applied Electrodynamics, Russian Academy of Sciences, Izhorskaya Str. 13, 125412 Moscow, Russia*
[5]*Institute of Applied Physics, Academy of Sciences of Moldova, Academiei Str. 5, MD-2028 Kishinev, Moldova*
[6]*Dipartimento di Fisica e Unifa CNISM, Universifa degli Studi di Parma, Vialle delle Scienze, 7A, 43100 Parma, Italy*
[7]*Institute of General and Inorganic Chemistry, Russian Academy of Sciences, Leninskiy pr. 31, 119991 Moscow, Russia*

(Received 23 October 2012; accepted 4 February 2013; published online 25 February 2013)

Structural and magnetic properties of the group III-V diluted magnetic semiconductor $In_{1-x}Mn_xSb$ with $x = 0.005$–0.06, including the nuclear magnetic resonance (NMR) investigations, are reported. Polycrystalline $In_{1-x}Mn_xSb$ samples were prepared by direct alloying of indium antimonide, manganese and antimony, followed by a fast cooling of the melt with a rate of 10–12 K/s. According to the X-ray diffraction data, part of Mn is substituted for In, forming the $In_{1-x}Mn_xSb$ matrix. Atomic force microscopy and scanning tunneling microscopy investigations provide evidence for the presence of microcrystalline MnSb inclusions (precipitates), having a size of ~100–600 nm, and the fine structure of nanosize grains with a Gaussian distribution around the diameter of ~24 nm. According to the NMR spectra, the majority of Mn enters the MnSb inclusions. In addition to the single Mn ions, which contribute to the magnetization M (T) only in the low-temperature limit of $T < 10$–20 K, and MnSb nanoprecipitates responsible for the ferromagnetic (FM) properties of $In_{1-x}Mn_xSb$, a superparamagnetic (SP) contribution of atomic-size magnetic Mn complexes (presumably dimers) has been established. The fraction of the MnSb phase, $\eta \sim 1$–4%, as well as the concentration, $n_{sp} \sim (0.8$–$3.2) \times 10^{19}$ cm^{-3}, and the magnetic moment of the Mn dimers, $\mu \sim 8$–$9\ \mu_B$, are determined. The solubility limit of Mn in the InSb matrix, $N_{SL} \sim 10^{20}$ cm^{-3}, is estimated. Hysteresis in low ($H < 500$ Oe) magnetic fields and saturation of the magnetization in high ($H > 20$ kOe) magnetic fields are observed, indicating a presence of the SP and FM contributions to the dependence of M (H) up to $T \sim 500$ K. The hysteresis is characterized by the coercivity field, H_c, decreasing between ~100 and 75 Oe when T is increased from 5 to 510 K. The values of H_c are in reasonable agreement with the effect of the largest MnSb inclusions. The maximum of M (T), measured in the zero-field-cooled and the field-cooled conditions in a weak field of 500 Oe, is observed at $T \sim 510$ K and is attributable to the Hopkinson effect. © *2013 American Institute of Physics*. [http://dx.doi.org/10.1063/1.4792652]

I. INTRODUCTION

$In_{1-x}Mn_xSb$, or briefly InMnSb, is a zinc blende compound belonging to the group III-V diluted magnetic semiconductors (DMS). Progress made in investigations of the group III-V Mn-doped DMS has demonstrated the high potential of these materials for use in spintronics applications.[1,2] However, the ferromagnetic (FM) Curie temperature, T_C, in these compounds still does not reach room temperature, as, for example, in substitutional $Ga_{1-x}Mn_xAs$ having $T_C \sim 200$ K.[3] Experimental and theoretical investigations have established both the intrinsic limitations for doping the group III-V semiconductors with Mn (Ref. 4) and the existence of an upper limit of T_C, lying well below room temperature for the majority of the group III-V DMS with carrier-mediated ferromagnetism.[5,6] On the other hand, substantial progress on this point is expected to be achieved by the alloying of the group III-V semiconductors with ferromagnetic compounds of the Mn-V type, such as MnAs and MnSb, which have $T_C = 317$ K and 585 K, respectively, in zero magnetic field.[7,8] In addition, the influence of small concentrations of MnAs inclusions on the coercivity field has been established in (Ga,Mn)As thin films.[9] Hysteresis of the anomalous Hall effect, depending on the hole concentration, was observed in (Ga,Mn)Sb films with MnSb precipitates, even above room temperature.[10] This implies that the FM properties of the (Ga,Mn)Sb films are not solely connected to the non-interacting MnSb nanoprecipitates. Indeed, the thickness of the Schottky barriers on the border of the MnSb nanoparticles and the host semiconductor matrix decreases as the hole concentration increases.

a)Present address: Institute of Solid State Physics, Vienna University of Technology, A -1040 Vienna, Austria.
b)Author to whom correspondence should be addressed. Electronic mail: erkki.lahderanta@lut.fi.

Therefore, the FM order, induced by the interaction of charge carriers with FM nanoparticles, appears when the thickness of the Schottky barriers becomes comparable with the hole wavelength.[10] This makes the interaction between the charge carriers and the FM nanoprecipitates important.

Indium antimonide (InSb) is known among the group III-V semiconductors as the material with the narrowest energy gap (0.18 eV), the highest carrier mobility (up to 7.8 $m^2\ V^{-1}\ s^{-1}$ at 300 K) and the largest spin-orbit coupling. In addition, investigations of InSb weakly doped with Mn (namely, at Mn concentration of less than $10^{19}\,cm^{-3}$) have demonstrated large negative magnetoresistance,[11] presumably related to the weak localization effects.[12]

The first FM $In_{1-x}Mn_xSb$ films having $T_C = 8.5$ K and 20 K at $x = 0.028$ (Ref. 13) and 0.1 (Ref. 14), respectively, were grown by the low-temperature molecular-beam epitaxy method. The FM state in these materials has presumably a carrier-mediated origin and influences the electronic transport as it is related to the Mn ions in the In sites.[13,15–18] According to theoretical investigations, the increase of the Mn concentration in InMnSb films does not lead to a strong increase of T_C. For example, the accurate mean-field calculations predict ferromagnetism of $In_{0.95}Mn_{0.05}Sb$ with $T_C < 40$ K at the itinerant hole concentration $p = 5 \times 10^{20}\,cm^{-3}$.[6]

However, a value of T_C as high as 130 K was obtained in bulk InMnSb synthesized by a controlled ambient annealing technique.[19] The FM transition above room temperature was observed in InMnSb films grown by pulsed laser deposition[20] and liquid phase epitaxy[21] and was also observed in bulk polycrystalline InMnSb.[22–24] On the other hand, experiments have shown that such high-temperature ferromagnetism in InSb heavily doped with Mn is due to the non-interacting MnSb precipitates but is not associated with the hole-mediated ferromagnetism.[21–23]

Observation of FM properties above room temperature has been reported recently in $In_{1-x}Mn_xSb$ with $x < 0.035$, grown by the metalorganic vapor phase epitaxy method.[25] Spin-dependent magnetotransport with the spin polarization ratio up to ~50% at 300 K was observed in a p-InMnSb/n-InSb magnetic semiconductor heterojunction, which was prepared in the same way.[26] In both cases, the ferromagnetism is attributable to magnetically active atomic-scale complexes (i.e., dimers or trimers) generated due to correlations of the spatial distribution of the Mn ions in In positions.[25] The existence of these kinds of complexes and their essential role in the formation of the FM state are widely discussed topic. Theoretical calculations for a system of (Ga,Mn)As have demonstrated the possibility of Mn clustering into stable and electronically active dimers, trimers, or tetramers.[27] Such complexes have been observed in InMnAs (Ref. 28) and in Ge:Mn (Ref. 29).

In this work, we investigate the structural and magnetic properties of InMnSb to clarify the role of various reasons for the formation of its magnetic state. In this connection, the following possible types of magnetic inclusions are analyzed: (i) the substitutional Mn ions in InSb, (ii) the MnSb precipitates, and (iii) the atomic-scale magnetic Mn complexes. InMnSb samples prepared by the direct melting of starting materials with a fast cooling rate were selected for the investigation.

II. EXPERIMENTAL DETAILS

Polycrystalline $In_{1-x}Mn_xSb$ samples with $x = 0.005$, 0.02, 0.03, and 0.06, containing 0.12, 0.5, 0.7, and 1.4 mass % of Mn, respectively, and labeled as # 1, # 2, # 3, and # 4, respectively, were prepared by direct melting of indium antimonide, manganese, and antimony. The components were prepared as powder with average particle sizes of 5–10 μm. The starting mixtures were weighed on a torsion balance with an accuracy of $\pm 1 \cdot 10^{-5}$ g. The samples were synthesized in evacuated (10^{-2} Pa) quartz ampules, etched in mixtures of analytical-grade HF, HCl, and HNO_3, washed with deionized water, kept at 400 K in a drying oven and coated with pyrolitic graphite. For improved homogenization, the synthesis temperature was 1048 K, or 250 K higher than the melting point of InSb (798 K), and the synthesis duration was 24 h. To overcome the solubility limit of Mn at equilibrium growth, fast cooling of the melt (10–12 K/s) was used. After synthesis, the growth ampoules contained only homogeneous boules having masses between 5 and 8 g. Therefore, in calculations, we used the initial mass of Mn as the total amount of Mn in samples. The composition and structure of the crystals were studied with three different methods: atomic absorption analysis, atomic force microscopy (AFM), and scanning electronic microscopy (SEM). The possible existence of minority phases was investigated by x-ray powder diffraction (XRD) analysis with DRON-1 diffractometer using Ni-filtered CuK_α radiation, having a 5% lower limit of detection. The temperature dependence of the magnetization, M (T), was measured with a SQUID magnetometer S600X (Cryogenic Ltd) separately between $T = 5$–310 K and $T = 260$–580 K, respectively, in magnetic fields up to $H = 50$ kOe. Nuclear magnetic resonance (NMR) spectra were obtained with a NMR spectrometer HyReSpect[30] using a tuned probe circuit. Frequency-swept spin-echo signals of ^{55}Mn, ^{121}Sb, and ^{123}Sb isotopes were investigated in the range of 180–450 MHz at different temperatures, both in zero and nonzero applied magnetic fields.

III. STRUCTURAL AND NMR INVESTIGATIONS

Only InSb peaks were detected in the XRD patterns of samples # 2, # 3, and # 4. The lattice constant a varies from 6.4794 Å in # 2 to 6.4779 Å in # 4. Because the atomic radii of Mn and In are 1.27 Å and 1.67 Å, respectively,[31] the decrease of a can be explained by the formation of $In_{1-x}Mn_xSb$ solid solutions when In is substituted by Mn in the In sites. This is in agreement with the p-type conductivity of the investigated material, because Mn acts as an acceptor when it occupies the In positions of the lattice.[2] Small traces of the secondary phases, attributable to compounds of the Mn-Sb family, have been observed earlier with the help of the synchrotron radiation method in InMnSb samples prepared in the same way.[23]

The AFM and SEM investigations presented in Fig. 1 reveal a formation of inclusions corresponding to the three-dimensional microcrystalline MnSb particles. The microcrystalline MnSb inclusions can be seen in Fig. 1(a) as black points. In particular, Fig. 1(a) demonstrates the polycrystalline structure of the sample and displays the region filled in with the MnSb precipitates. However, the lateral distribution

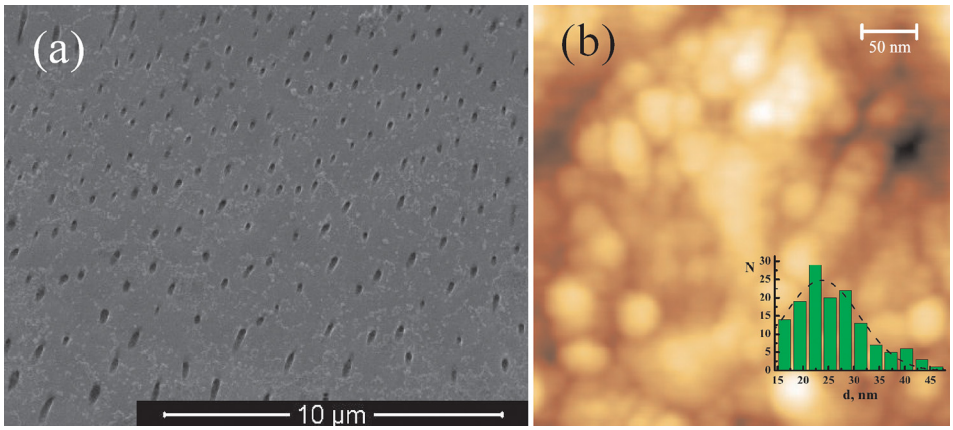

FIG. 1. SEM image of # 4 displaying precipitates, embedded in the host InMnSb matrix (a). AFM image of # 4 with the fine structure of the precipitates composed of nanograins (nanoparticles) (b). Inset: The distribution function of the nanograin diameter, fitted with the Gaussian function (the dashed line).

of these precipitates is not uniform, including some regions with very small particle concentrations. The lateral size of the MnSb precipitates varies between ~100 and 600 nm. In Fig. 1(b), one of the precipitates is displayed on an enlarged scale, showing the fine structure. The MnSb precipitates are composed of nanograins with a mean size of ~24 nm, and they have a Gaussian distribution of the nanograin diameter (see the inset to Fig. 1(b)). A similar structure of the InMnSb alloys was observed earlier.[22,32]

The presence of MnSb nanoprecipitates in the samples is confirmed by zero-field NMR measurements. The NMR spectrum of # 3 at $T = 2$ K is shown in Fig. 2. It should be noted here that very similar spectra were observed in the samples with different Mn concentrations, indicating that the position of these lines does not depend on the Mn content. We detected three distinct resonance lines centered at frequencies of $f_1 \approx 223$ MHz, $f_2 \approx 260$ MHz, and $f_3 \approx 420$ MHz. The ratio of two of the resonance frequencies is $f_3/f_1 \approx 1.88$, which corresponds within experimental error to the relation of the gyromagnetic ratios, $^{121}\gamma/^{123}\gamma = 1.84$. Therefore, the peaks at f_3 and f_1 can be associated with ^{121}Sb and ^{123}Sb, respectively, with the same internal hyperfine field. The rather sharp line at f_2 is attributable to ^{55}Mn. This assignment is corroborated by the shifts of the NMR peaks in the applied magnetic field

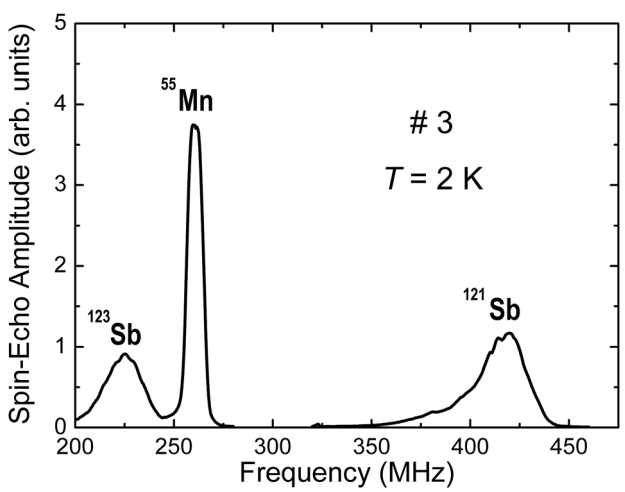

FIG. 2. Zero-field NMR spin-echo spectrum for # 3 measured at $T = 2$ K. The three distinct lines at 223 MHz, 260 MHz, and 420 MHz are attributed to ^{123}Sb, ^{55}Mn, and ^{121}Sb, respectively.

(data not shown). The lines at f_1 and f_3 are shifted to higher frequencies, indicating a positive (i.e., parallel to the magnetization) hyperfine field on Sb ions. On the other hand, the line at f_2 is shifted to lower frequencies, as expected for the negative hyperfine field of the Mn ions.[33] The intensity of all peaks is reduced with respect to the zero field spectra, which is characteristic of ferromagnetically enhanced NMR lines.[34]

The main contribution to the local field at the nuclei of magnetic atoms or ions comes from the spin-polarized bound and collective *s*-electrons. The spin polarization of these electrons arises from an exchange interaction with the ordered electron spins. Due to the collective electrons and to the overlapping of the wave functions of adjacent atoms, the spin polarization of magnetic materials is transferred from magnetic ions to nonmagnetic atoms, giving rise to hyperfine fields of the Fermi-contact origin on their nuclei. Therefore, the NMR frequency of the magnetic and nonmagnetic ions in zero magnetic field strongly depends on the magnetic and conducting state of the compound. MnSb is an intermetallic compound with a hexagonal NiAs-type structure, while InMnSb is the diluted magnetic semiconductor with zinc blende structure. This means that the spin state of bound and collective *s*-electrons in MnSb is quite different from that of $In_{1-x}Mn_xSb$. Hence, if the Mn atoms replace the In ions in the semiconductor matrix of InSb in random, the ^{55}Mn resonance frequency should differ from that of MnSb. However, the ^{55}Mn spectrum in our InMnSb samples and in MnSb (Ref. 35) is identical, demonstrating its connection to MnSb magnetic precipitates in the semiconductor matrix. The absence of any other magnetic Mn resonance line reveals a phase separation of the InMnSb samples into InSb (with minority of Mn) and MnSb. It is worth mentioning that the relatively high ^{55}Mn NMR sensitivity, $^{55}\gamma = 10.501$ MHz/T, and the 100% abundance of ^{55}Mn, as well as the NMR signal enhancement in ferromagnetic materials make it possible to detect MnSb particles of a few tens of nanometers, which are randomly distributed in a matrix.[34] In addition, an increase of x from 0.03 to 0.06 doubles the integrated NMR intensity. Hence, we can conclude that the majority of Mn atoms reside within the MnSb nanoprecipitates rather than substitute randomly for the In ions in the InSb host.

To summarize, the structural and NMR investigations above demonstrate that (i) only a minority of Mn can occupy the In positions, forming the $In_{1-x}Mn_xSb$ matrix, and (ii) the

majority of Mn ions are confined into the MnSb grains (particles), embedded in the matrix above. Additionally, possible existence of the Mn complexes (dimers and trimers) of atomic size should be taken into account.[25] Generally, this kind of distribution of Mn looks typical of InMnSb. It should be stressed that the results of Ref. 25 provide strong evidence for the Mn complexes above, playing an essential role in the magnetic properties of the $In_{1-x}Mn_xSb$ films. The coincidence of T_C in the $In_{1-x}Mn_xSb$ films ($T_C = 590$ K)[25] and in MnSb ($T_C = 585$ K)[8] points to the MnSb nanoprecipitates as a possible source of the high-temperature ferromagnetism in $In_{1-x}Mn_xSb$. However, despite our results above, no evidence of any secondary phase in the InMnSb layer was observed in Ref. 25 by XRD study or by the high-resolution transmission electron microscopy (TEM) method. On the other hand, the secondary phase was detected by the same group and reported in Ref. 36, published before Ref. 25. Eventually, the MnSb nanoinclusions were observed in high-temperature FM $In_{1-x}Mn_xSb$ semiconductor films with $x > 0.08$, deposited by metalorganic vapor phase epitaxy, and reported quite recently.[37] The reason for such a high Curie temperature coinciding with that of MnSb in the absence of the MnSb grains, detected by TEM, is not clear.[38] In this paper, we show that the role of each of the three Mn-based magnetic inclusions described above in the formation of the magnetic state of InMnSb can be further clarified by a detailed analysis of the magnetization.

IV. MAGNETIZATION

The temperature dependence of the magnetization at 50 kOe is exhibited in Fig. 3 for all the investigated samples. There are two noticeable features of the magnetization curves in Fig. 3: (i) a rapid increase of M (T) in the low-temperature (below ~20 K) and high-temperature (above ~500 K) intervals, and (ii) the region of the relatively weak variation of M (T) between $T \sim 50 - 500$ K. The high-temperature interval of M (T) resembles the FM transition or behavior near T_C. Because the temperature of our measurements is limited to 580 K, T_C can be estimated to lie slightly above 600 K.

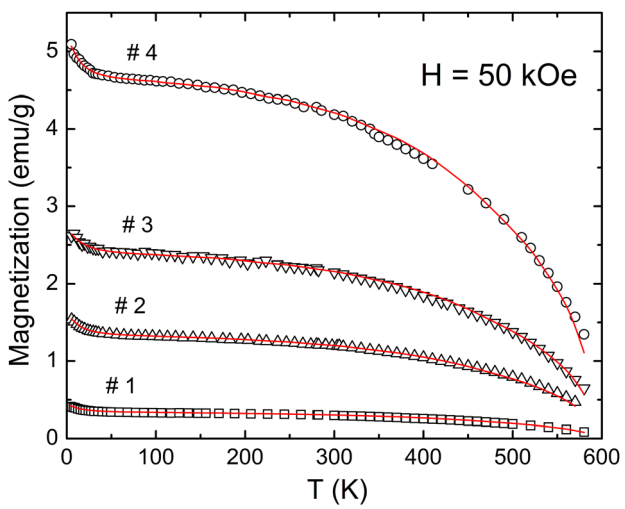

FIG. 3. Temperature dependence of the magnetization in the magnetic field of 50 kOe.

A similar low-temperature upturn of the magnetization was also observed in the epitaxial (In,Mn)Sb (Ref. 25), (Ga,Mn)As (Ref. 9), and Ge:Mn (Ref. 29). Usually, the increase of M (T) at $T \to 0$ is attributed to the FM transition connected to Mn in the matrix. The low-temperature FM transition in a system of Mn ions in the In positions of the (In,Mn)Sb matrix was observed earlier in the MBE grown samples,[13,16] and in our samples it appears to occur at $T < 20$ K (see above). Therefore, to clarify the role of the remaining two important magnetic units, namely, the MnSb nanoparticles and the atomic-size Mn complexes, we analyze here the M (T) dependence only above 20 K.

The behavior of the magnetization in our material can be explained by two coexisting magnetic phases. The first phase yields a paramagnetic (PM) or superparamagnetic (SP) contribution, M_{sp}, described by the Langevin function[39] and is referred to below simply as SP. The second phase is attributable to the MnSb nanoprecipitates and provides a ferromagnetic contribution, M_f, which is expected to dominate in the high-temperature interval. Therefore, the total magnetization can be described with the expression

$$M(T) = M_{sp}(T) + M_f(T) = M_{sp0}\left[\text{cotanh}\left(\frac{\mu H}{kT}\right) - \frac{kT}{\mu H}\right] + \eta M_{MnSb}(T), \quad (1)$$

where $M_{sp0} = n_{sp}\mu$ is the saturation magnetization of the SP subsystem, n_{sp} is the concentration of the SP particles, μ is the effective magnetic moment of a particle, η is the fraction of the MnSb phase, and M_{MnSb} (T) is the temperature-dependent saturation magnetization of MnSb. The function M_{MnSb} (T) was found by interpolation of the basic data in Ref. 8.

Equation (1) is reduced to the expression M (T) ~ M_f (T) = $\eta M_{MnSb}(T)$ at high temperatures, which makes it possible to obtain η for all samples and to fit the experimental data between 20 and 600 K in Fig. 3 with Eq. (1), using only two adjustable parameters, M_{sp0} and μ. The results of the fitting are displayed in Fig. 3 (solid lines) and the values of η, M_{sp0}, μ and n_{sp} are collected in Table I.

The values of η in Table I correlate well with Fig. 1(a), since the MnSb grains or black dots in Fig. 1(a) occupy only a small part of the sample volume. With the values of η and the amounts of Mn used in the preparation process, we evaluated the concentrations of the Mn ions, n_{Mn}, incorporated into the InSb lattice. The n_{Mn} value tends toward saturation, as can be seen in Fig. 4. It should be mentioned that n_{Mn} is smaller than the Mn content, obtained from the value of η, by the factors 5 and 7 for # 3 and 4, respectively. This is in agreement with the NMR investigations above (see Sec. III), namely, with the conclusion that the majority of Mn resides within MnSb nanoprecipitates. This permits us to estimate the solubility limit of Mn in InSb, $N_{SL} \sim 10^{20}$ cm^{-3}, for the preparation method of InMnSb used in our work. The value of N_{SL} is on the order of a magnitude higher than the solid solubility of Mn in bulk InSb crystals, $5 \times 10^{18} - 1 \times 10^{19}$ cm^{-3} (Ref. 40) but is ~5 times lower than the Mn content in the $In_{1-x}Mn_xSb$ epitaxial films [25].

The Curie temperature in our samples is estimated to be slightly above 600 K, exceeding $T_C = 585$ K for the bulk

TABLE I. The Mn content and composition (x) of $In_{1-x}Mn_xSb$ samples, the mass and the volume fractions of the MnSb phase (η), the saturation magnetization of the SP subsystem (M_{sp0}), the magnetic moment (μ) and the concentration (n_{sp}) of the SP particles.

Sample No.	Mn content mass %	Composition x	η mass %	η vol. %	M_{sp0} emu/g	μ μ_B	n_{sp} cm^{-3}
1	0.12	0.005	0.3	0.25	0.11	8.4 ± 0.4	8.2×10^{18}
2	0.5	0.02	1.2	1.0	0.28	8.8 ± 0.4	1.9×10^{19}
3	0.7	0.03	1.85	1.6	0.36	9.4 ± 1.2	2.4×10^{19}
4	1.4	0.06	4.1	3.5	0.41	8.1 ± 0.4	3.2×10^{19}

MnSb (Ref. 8). This difference is attributable to the different Mn content in the bulk and grain MnSb or to the importance of the surface effects in the MnSb particles (grains).

The temperature dependence of the SP part of the magnetization is displayed in Fig. 5. As can be seen from the inset to Fig. 5, the dependence of M_{sp} (T) is close to the Curie law in agreement with its PM or SP nature. In this figure, the data obtained at $T < 10$ K are omitted, violating the expansion of the function cotanh (x) $\sim 1/x + x/3 + \cdots$ which leads to the Curie or the Curie-Weiss law only for $x \ll 1$. Such an omission is also substantiated by the FM transition inside the $In_{1-x}Mn_xSb$ matrix,[13,16] which is expected to be at the lowest temperatures, as discussed above.

The SP contribution to the magnetization can be connected to the single-domain MnSb particles with a diameter of less than 15 nm, to single Mn ions or to Mn complexes of atomic sizes (dimers or trimers). However, the contribution of single-domain MnSb nanoparticles is unlikely because of their concentration of $\sim 10^{15}$ cm^{-3}, which is much smaller than those of n_{sp} in Table I. In addition, the magnetic moment of the SP particles lying around $\sim 9\mu_B$ (Table I) is incomparable with a typical magnetization of single-domain magnetic particles.[39] On the other hand, the moment of Mn^{2+} ($S = 5/2$) occupying an In site is close to $5\mu_B$, as has been found in the $In_{1-x}Mn_xSb$ epitaxial films.[13] This value is about 2 times smaller than those of μ in Table I. Taking into account the above consideration, it is possible to attribute the SP response to the small magnetic clusters or Mn complexes of atomic size mentioned in Secs. I and III. Indeed, the theoretical investigations of a similar (Ga,Mn)As system predicted the possibility of Mn clustering into stable and electronically active dimers, trimers, or tetramers.[27] Such complexes were observed in InMnAs (Ref. 28) and (In,Mn)Sb epitaxial films,[25] as well as in Ge:Mn (Ref. 29). On the other hand, as can be seen in Fig. 4, the values of n_{sp} are $\sim$3 times smaller than those of n_{Mn}. This gives strong support to the existence of the Mn complexes, especially dimers and trimers, in our material. Taking into account that not all Mn atoms occupying In sites enter such complexes, it is reasonable to assume that these complexes are mainly dimers. Furthermore, some of the Mn atoms inside the InSb lattice are magnetically inactive, which diminishes the n_{sp}/n_{Mn} ratio as well. The value of $\mu \sim 9\mu_B$ is also supported by the assumption that the majority of the atomic-size magnetic complexes in our samples are represented by dimers.

The temperature dependence of the magnetization of # 4 in the low field of 500 Oe, measured after cooling in zero magnetic field (zero-field-cooled or ZFC) and non-zero magnetic field (field-cooled or FC), M_{ZFC} (T) and M_{FC} (T), respectively, is shown in Fig. 6. Both the ZFC and the FC data exhibit a clear maximum at $\sim$510 K. A similar behavior of M_{ZFC} (T) is usually observed in systems with a frustrated ground magnetic state, e.g., in spin glasses or cluster glasses.[41] However, because M_{FC} (T) does not have a maximum in glassy systems,[41] the behavior shown in Fig. 6 is instead attributable to the manifestation of the Hopkinson effect.[42] This effect can be observed in not very small single-domain particles and is connected to the competition between temperature dependences of the saturation

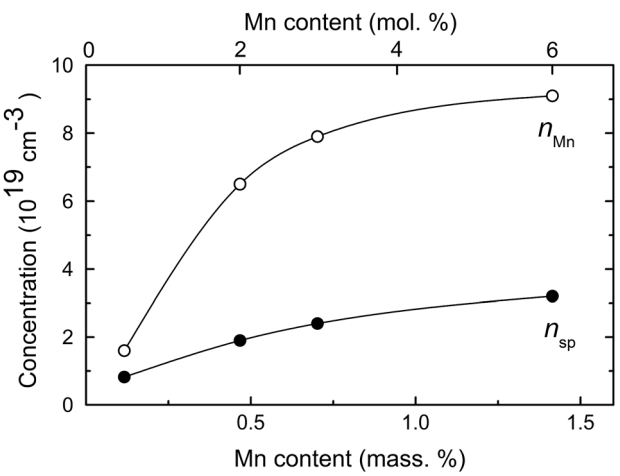

FIG. 4. The concentration of Mn substituting for In in the $In_{1-x}Mn_xSb$ lattice, n_{Mn} (open circles), and the concentration of the SP particles, n_{sp} (solid circles), plotted as the functions of the Mn content. The lines are to guide the eye.

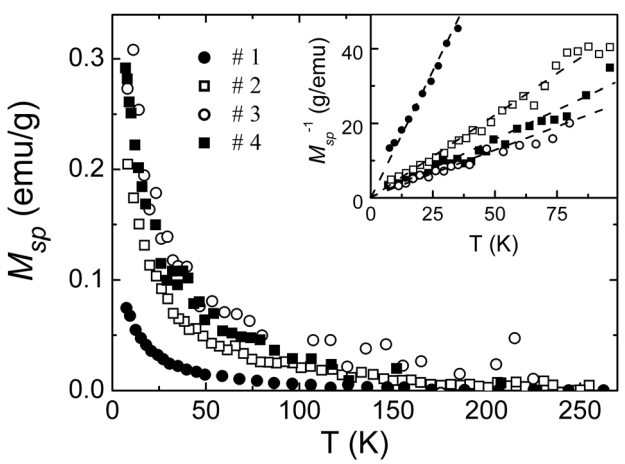

FIG. 5. Temperature dependence of the SP contribution, M_{sp}, to the net magnetization. Inset: The plots of M_{sp}^{-1} vs. T. The dashed lines are to guide the eye.

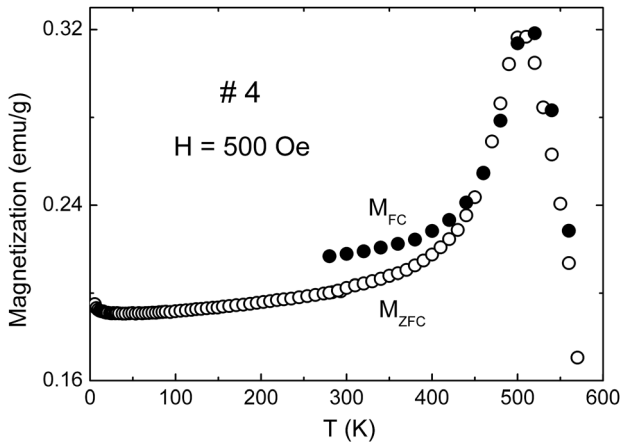

FIG. 6. Temperature dependences of M_{ZFC} (open circles) and M_{FC} (solid circles) for # 4 at H = 500 Oe.

magnetization and the anisotropy field. The magnetization of a system of randomly oriented particles in a low magnetic field is given by the expression $M_{rs}\ (T) \sim M_s\ (T)/H_a\ (T)$, where $M_s\ (T)$ is the bulk saturation magnetization and $H_a\ (T)$ is the anisotropy field of particles. When T increases, $H_a\ (T)$ decreases which leads to spin reorientation from the easy direction to the hard direction of the magnetization. This stimulates an overall increase of the magnetization, which reaches a maximum below T_C (the Hopkinson peak), provided that $H_a\ (T)$ decreases faster than $M_s\ (T)$.[42]

The existence of the SP particles in our samples is also supported by the field dependences of the magnetization, $M\ (H)$, as shown for # 4 in Fig. 7. It can be seen that the saturation of the magnetization in the highest magnetic fields is incomplete, whereas the dependence $M\ (H)$ resembles that in the SP materials. The behavior of $M\ (H)$ in other samples is similar to that shown in Fig. 7. However, the magnetic field dependence of the magnetization cannot be described only by a classical model of superparamagnetism (as provided by the Langevin function),[39] because the $M\ (H)$ curves, measured at different temperatures, do not exhibit the H/T scaling. The hysteresis in low fields (see the inset to Fig. 7) reveals

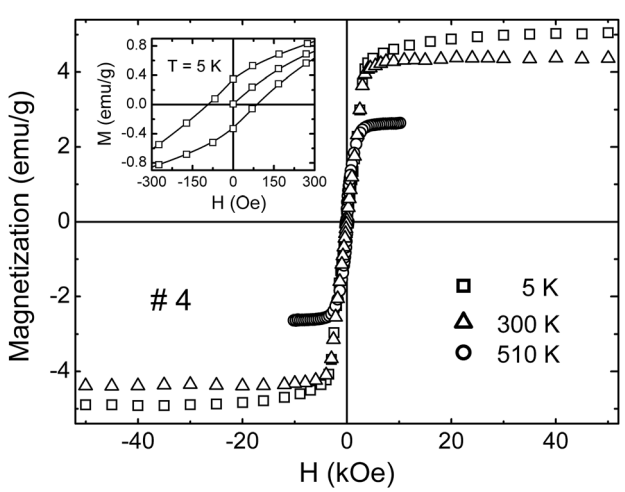

FIG. 7. The dependence of the magnetization on the magnetic field for # 4 at $T = 5$, 300 K and 510 K. Inset: A part of the low-field hysteresis loop at $T = 5$ K.

the presence of the FM contribution, attributable to sufficiently large MnSb inclusions. The coercive force, H_c, is found to be ~100 Oe at 5 K (refer to the inset to Fig 7) and decreases down to ~70 Oe when T is increased up to 510 K. On the other hand, the coercive force can be estimated with the expression $H_c \sim (4\pi/3)\ M_s$, where M_s is the saturation magnetization of the FM subsystem. With this expression, one finds $H_c \sim 75$ Oe and 50 Oe at $T = 5$ K and 510 K, respectively, which is quite comparable to the experimental data. For samples # 3 and # 4, the value of $H_c \sim 50$ Oe is found. On the other hand, samples containing MnSb particles with the mean diameter ~15 nm and 30 nm exhibit FM behavior with the values of $H_c \sim 6500$ and 4500 Oe, respectively (Ref. 43), which is decreased to $H_c \sim 300$ Oe for the particles of micrometer size (Ref. 44). Therefore, the reduced coercivity in our samples is attributable to a weak coupling between the FM MnSb particles due to their large size and low concentration.

V. CONCLUSIONS

We have performed structural, NMR and magnetization investigations of polycrystalline InMnSb samples with different Mn content ($x = 0.005$, 0.02, 0.03, and 0.06). The XRD data reveal a decrease of the lattice constant corresponding to increasing Mn concentration, indicating a partial substitution of Mn for In in the InSb lattice. The SEM images provide evidence for the presence of three-dimensional microcrystalline MnSb inclusions (precipitates) with the size of ~100−600 nm embedded into the $In_{1-x}Mn_xSb$ matrix. The fine structure of the MnSb precipitates, which has been established with the SEM investigations, consists of nanograins with a Gaussian size distribution around a diameter ~ 24 nm. The NMR spectra of InMnSb support the presence of the MnSb nanoprecipitates and give evidence that the majority of Mn enters them.

These structures show ferromagnetic behavior up to 585 K. Analysis of the temperature dependence of the magnetization reveals three types of magnetic species: (i) the substitutional Mn ions making the PM contribution below ~ 10−20 K, (ii) the MnAs precipitates governing the FM properties of the material, and (iii) the atomic-size Mn complexes (presumably dimers with the magnetic moment ~9 μ_B) responsible for the SP contribution to $M\ (B)$. The concentrations for each type of the magnetic inclusions above are obtained. They range between 2×10^{19} and 9×10^{19} cm^{-3} for single Mn ions substituting In and between 8×10^{18} and 3×10^{19} cm^{-3} for Mn complexes of atomic size, whereas the volume fraction of MnAs varies between 0.25 and 3.5%. The solubility limit of Mn in the InSb matrix is estimated to be ~ 10^{20} cm^{-3}, which exceeds considerably the values in bulk crystals, $5 \times 10^{18} - 1 \times 10^{19}$ cm^{-3} (Ref. 39), but is ~5 times lower than in epitaxial films of $In_{1-x}Mn_xSb$ (Ref. 25).

The dependence $M\ (B)$ exhibits a clear hysteresis in low fields and saturation in high fields, indicating the presence of the SP and the FM responses. The FM contribution is attributable to the largest MnSb inclusions, which is in agreement with the estimated values of the coercivity field. The maximum of the dependences $M_{ZFC}\ (T)$ and $M_{FC}\ (T)$, observed in a weak magnetic field, is interpreted by the Hopkinson effect.

ACKNOWLEDGMENTS

We are indebted to Mr. A. V. Molchanov and Dr. S. G. Mikhailov for their assistance in sample preparation. This work was supported by the Russian Foundation of Basic Research (RFBR) with Grant Nos. 10-03-00666 and 11-02-00363 and by the Ministry of Education and Science of the Russian Federation with Grant No. 3.5536.2011. B. A. Aronzon is grateful to the RFBR (Russian—Israeli Grant No. 11-02-92478) for financial support and to Professor A. Gerber for fruitful discussions.

[1]T. Jungwirth, J. Sinova, J. Masek, J. Kucera, and A. H. MacDonald, Rev. Mod. Phys. **78**, 809 (2006).
[2]I. Zutic, J. Fabian, and S. Das Sarma, Rev. Mod. Phys. **76**, 323 (2004).
[3]L. Chen, X. Yang, F. Yang, J. Zhao, J. Misuraca, P. Xiong, and S. von Molnar, Nano Lett. **11**, 2584 (2011).
[4]W. Walukiewicz, Physica B **302–303**, 123 (2001).
[5]K. M. Yu, W. Walukiewicz, T. Wojtowicz, M. W. Lim, X Liu, U. Bindley, M. Dobrowolska, and J. K. Furduna, Phys. Rev. B **68**, 041308(R) (2003).
[6]T. Jungwirth, J. Konig, J. Sinova, and A. H. MacDonald, Phys. Rev. B **66**, 012402 (2002).
[7]L. Pytlik and A. Zieba, J. Magn. Magn. Mater. **51**, 199 (1985).
[8]W. J. Takei, D. E. Cox, and G. Shirane, Phys. Rev. **129**, 2008 (1963).
[9]K. Y. Wang, M. Sawicki, K. W. Edmonds, R. P. Campion, A. W. Rushforth, A. A. Freeman, C. T. Foxon, B. L. Gallagher, and T. Dietl, Appl. Phys. Lett. **88**, 022510 (2006).
[10]V. V. Rylkov, B. A. Aronzon, Yu. A. Danilov, Yu. N. Drozdov, V. P. Lesnikov, K. I. Maslakov, and V. V. Podolskii, JETP **100**, 742 (2005).
[11]S. A. Obukhov, B. S. Neganov, Yu. S. Kiselev, A. N. Chernikov, V. S. Vekshina, N. I. Pepik, and A. N. Popkov, Cryogenics **31**, 874 (1991).
[12]P. A. Lee and T. V. Ramakrishnan, Rev. Mod. Phys. **57**, 287 (1985); B. L. Altshuler and A. G. Aronov, in *Electron-Electron Interaction in Disordered Systems*, edited by A. L. Efros and M. Pollak (North-Holland, Amsterdam, 1985), p.155.
[13]T. Wojtowicz, G. Cywinski, W. L. Lim, X. Liu, M. Dobrowolska, J. K. Furduna, K. M. Yu, W. Walukiewicz, G. B. Kim, M. Cheon, X. Chen, S. M. Wang, and H. Luo, Appl. Phys. Lett. **82**, 4310 (2003).
[14]S. Yanagi, K. Kuga, T. Slupinski, and H. Munekata, Physica E **20**, 333 (2004).
[15]X. Chen, M. Na, M. Cheon, S. Wang, H. Luo, D. McComb, X. Liu, Y. Sasaki, T. Wojtowicz, J. K. Furduna, S. G. Potashnik, and P. Schiffer, Appl. Phys. Lett. **81**, 511 (2002).
[16]G. Mihaly, M. Csontos, S. Bordacs, I. Kezsmarki, T. Wojtowicz, X. Liu, B. Janko, and J. K. Furduna, Phys. Rev. Lett. **100**, 107201 (2008).
[17]M. Csontos, T. Wojtowicz, X. Liu, M. Dobrovolska, B. Janko, J. K. Furduna, and G. Mihaly, Phys. Rev. Lett. **95**, 227203 (2005).
[18]M. Csontos, G. Mihaly, B. Janko, T. Wojtowicz, X. Liu, and J. K. Furduna, Nature Mater. **4**, 447 (2005).
[19]J. Hollingswort and P. R. Bandaru, Mater. Sci. Eng. B **151**, 152 (2008).
[20]Yu. A. Danilov, E. S. Demidov, Yu. N. Drosdov, V. P. Lesnikov, V. V. Podolski, M. V. Sapozhnikov, and A. P. Kasatkin, J. Magn. Magn. Mater. **300**, e24 (2006).
[21]K. Ganesan, S. Mariyappan, and H. L. Bhat, Solid State Commun. **143**, 272 (2007).
[22]K. Ganesan and H. L. Bhat, J. Appl. Phys. **103**, 043701 (2008).
[23]V. M. Novotortsev, I. S. Zakharov, A. V. Kochura, S. F. Marenkin, R. Laiho, E. Lahderanta, A. Lashkul, A. G. Veresov, A. V. Molchanov, and G. S. Yur'ev, Russian J. Inorg. Chem. **51**, 1627 (2006).
[24]V. A. Ivanov, O. N. Pashkova, E. A. Ugolkova, V. P. Sanygin, and R. M. Galera, Inorg. Mater. **44**, 1041 (2008).
[25]N. D. Parashar, N. Rangaraju., V. K. Lazarov, S. Xie, and B. W. Wessels, Phys. Rev. B **81**, 115321 (2010).
[26]J. A. Peters, N. Rangaraju, C. Feeser, and B. W. Wessels, Appl. Phys. Lett. **98**, 193506 (2011).
[27]H. Raebiger, A. Ayuela, and J. von Boehm, Phys. Rev. B. **72**, 014465 (2005).
[28]Y. L. Soo, S. Kim, Y. H. Kao, A. J. Blattner, B. W. Wessels, S. Khalid, C. Sanchez Hanke, and C. C. Kao, Appl. Phys. Lett. **84**, 481 (2004).
[29]C. Jaeger, C. Bihler, T. Valliatis, S. T. B. Coennenwein, M. Opel, R. Gross, and M. S. Brandt, Phys. Rev. B **74**, 045330 (2006).
[30]G. Allodi, A. Banderini, R. De Renzi, and C. Vignali, Rev. Sci. Instrum.**76**, 83911 (2005).
[31]J. A. Dean, *Lange's Handbook of chemistry*, 15th ed. (McGraw-Hill, New York, 1999), pp. 4.30–4.34.
[32]L. Rednic, I. G. Deac, E. Dorolti, M. Coldea, V. Rednic, and M. Neumann, Cent. Eur. J. Phys. **8**, 620 (2010).
[33]A. J. Freeman and R. E. Watson, *Magnetism*, edited G. T. Rado and H. Suhl (Academic, New York and London, 1965), Vol. 2 A, p. 168.
[34]M. I. Kurkin and E. A. Turov, *NMR in Magnetically Ordered Materials and Its Applications* (Nauka, Moscow, 1990).
[35]A. Tsujimura, T. Hihara, and Y. Koi, J. Phys. Soc. Jpn. **17**, 1078 (1962); T. Rajasekharan and K. V. S. Rama Rao, Phys. Status Solidi A **50**, 303 (1978); K. Le Dang, P. Veillet, P. Beauvillain, N. Nakayama, and T. Shinjou, J. Phys.: Condens. Matter **1**, 6153 (1989).
[36]N. D. Parashar, D. J. Keavney, and B. W. Wessels, Appl. Phys. Lett. **95**, 201905 (2009).
[37]C. E. Feeser, L. Lari, V. K. Lazarov, J. A. Peters, and B. W. Wessels, J. Vac. Sci. Technol. B. **30**, 032801 (2012).
[38]A small mass fraction of the MnSb phase and its non-uniform distribution could be the reasons for the lacking of its observation in Ref. 25. In addition, formation of MnSb precipitates is stimulated, generally, by the overall increase of the Mn content in InMnSb epitaxial films.
[39]C. P. Bean and J. D. Livingston, J. Appl. Phys. **30**, 120S (1959).
[40]M. Y. Dashevskii, V. S. Ivleva, L. Y. Krol, I. N. Kurilenko, L. B. Litvak-Gorskaya, R. S. Mitrofanova, and E. Y. Fridlyand, Sov. Phys. Semicond. **5**, 757 (1971).
[41]D. Chowdhury, *Spin Glasses and Other Frustrated Systems* (World Scientific, Singapore, 1986); S. L. Ginzburg, *Irreversible Phenomena of Spin Glasses* (Nauka, Moscow, 1989).
[42]S. Prasad and N. S. Gajbhiye, J. Alloys Compd. **265**, 87 (1998).
[43]H. Zhang, S. S. Kushvaha, S. Chen, X. Gao, D. Qi, A. T. S. Wee, and X.-S. Wang, Appl. Phys. Lett. **90**, 202503 (2007).
[44]B. L. Low, C. K. Ong, J. Lim, A. C. H. Huan, H. Gong, and T. Y. F. Liew, J. Appl. Phys. **85**, 7340 (1999).